Quasi-phase-matched 1.064-μm-pumped optical parametric oscillator in bulk periodically poled $LiNbO_3$

L. E. Myers, G. D. Miller, R. C. Eckardt, M. M. Fejer, and R. L. Byer

E. L. Ginzton Laboratory, Stanford University, Stanford, California 94305

W. R. Bosenberg

Lightwave Electronics Corporation, Mountain View, California 94043

Received August 29, 1994

We report a quasi-phase-matched optical parametric oscillator, using bulk periodically poled $LiNbO_3$. The optical parametric oscillator, pumped by a 1.064-μm Q-switched Nd:YAG laser, was temperature tuned over the wavelength range 1.66–2.95 μm. The oscillation threshold of $\approx$0.1 mJ was more than a factor of 10 below the damage limit. The $LiNbO_3$ crystal, fabricated by application of an electric field to a sample with liquid and metal surface electrodes, was 0.5 mm thick with a 5.2-mm interaction length and a quasi-phase-matched period of 31 μm.

In this Letter we report an optical parametric oscillator (OPO), using quasi-phase matching (QPM) in a bulk nonlinear optical material, periodically poled $LiNbO_3$ (PPLN). QPM is an alternative technique to birefringent phase matching for compensating phase velocity dispersion in frequency-conversion applications.[1] In a QPM device the nonlinear coefficient is modulated with a period twice the coherence length of the interaction to offset the accumulated phase mismatch. QPM can be implemented in a ferroelectric material, such as $LiNbO_3$, by periodic reversal of the ferroelectric domains, since antiparallel domains correspond to a sign reversal of the nonlinear coefficient. A significant advantage of QPM is that any interaction within the transparency range of the material can be noncritically phase matched at a specific temperature. Another benefit is that the interacting waves can be chosen so that coupling occurs through the largest element of the $\chi^{(2)}$ tensor. In $LiNbO_3$, QPM with all waves polarized parallel to the z axis yields a gain enhancement over the birefringently phase-matched process of $(2d_{33}/\pi d_{31})^2 \approx 20$.

Implementation of QPM requires a fabrication method that can achieve uniform micrometer-scale periodic structures while preserving the material's transparency, nonlinearity, and power-handling capability. QPM was proposed before birefringent phase matching,[2] but difficulties in fabricating QPM materials have prevented its widespread use. Recent advances in fabricating practical QPM materials have renewed interest in this approach. $LiNbO_3$ has attracted special attention because it is a mature, readily available material with transparency covering a useful range from 0.35 to >4 μm. Several techniques have been developed for producing PPLN. Chemical indiffusion has been used to make periodic structures of good quality; however, the pattern is limited to shallow layers only sufficient for waveguide devices, and the structure lacks the power-handling capability required for many applications.[3] Bulk PPLN has been made by modulation of the crystal growth process, but it suffers from axial variations in domain periodicity that significantly degrade efficiency.[4,5] Electron beam writing can produce bulk PPLN with good periodicity, but uniformity is poor and the process does not lend itself to manufacturability.[6] Recently, techniques for ferroelectric domain reversal with an external electric field have produced PPLN for QPM second-harmonic generation.[7,8] In this approach, domain periodicity is precisely defined by a lithographic mask by use of standard microfabrication techniques. We have developed an electric-field poling process that yields uniform PPLN in thick substrates for efficient QPM frequency-conversion applications.

We used standard 0.5-mm-thick optical-grade $LiNbO_3$ wafers of congruent composition. For the positive electrode, we deposited a 200-nm-thick aluminum grating on the $+z$ surface using lift-off lithography. A 2-μm-thick layer of photoresist was applied over the grating, leaving the edge of the metal pattern exposed. Contact was made to the exposed metal with a liquid electrolyte consisting of lithium chloride in deionized water. The photoresist layer insulated the electrode lines, inhibited domain growth between the grating lines, and formed the contour of an isopotential surface when covered with the electrolyte. The isopotential surface controlled fringing fields at the edges of the grating lines, improving pattern uniformity and resolution. We also patterned the $+z$ surface directly with photoresist trenches and liquid contact,[9] but we found that metal lines provided better pattern fidelity and the metal–$LiNbO_3$ contact enhanced the poling in that region. For the negative electrode, liquid electrolyte was applied directly to the bare $-z$ surface. The liquid electrode fixture consisted of two electrolyte-containing chambers that squeezed the $LiNbO_3$ sample between O-rings. This arrangement permitted application of fields exceeding 25 kV/mm

0146-9592/95/010052-03$6.00/0

without breakdown of the sample and without the need for surrounding oil or vacuum.

The poling circuit consisted of a high-voltage amplifier with a series resistor to regulate the current. Domain reversal required a field strength exceeding 21 kV/mm at room temperature. A current of 13 to 33 μA was used to pole the devices reported in this Letter. Testing was also performed at currents up to 10 mA, but the lower current tended to produce straighter domain walls. The duration of the poling current depended linearly on the area being poled. The charge Q transferred to the sample was that required to compensate the reversed orientation of the spontaneous polarization, given by $Q = 2P_S A$, where $P_S = 0.71$ C/m^2 is the spontaneous polarization of $LiNbO_3$, A is the area of the domain-reversed region, and the factor of 2 accounts for the polarity reversal. For the devices reported here, poling times ranged from 0.36 to 1.9 s. Shown in Fig. 1 is a cross-sectional view of a PPLN sample, illustrating the straight, vertical domain boundary walls throughout the material volume.

To verify domain pattern homogeneity for infrared parametric interactions, we performed a difference-frequency-generation experiment, using another sample with 15.5-μm grating period similar to that shown in Fig. 1. The end faces of the crystal were polished down to the periodically poled region such that the finished device was 2.2 mm long. Pump radiation from a cw Ti:sapphire tunable near 710 nm and signal radiation from a 1.555-μm cw erbium fiber laser were mixed in the PPLN crystal. The single-pass idler power generated near 1.3 μm is shown in Fig. 2, along with the theoretical tuning curve. The ripples in the measured data are due to interference effects of Fresnel reflections from the uncoated polished end faces of the crystal. The bandwidth of the theoretical curve is as calculated from the Sellmeier coefficients for bulk $LiNbO_3$ at room temperature[10]; the phase-matching peak has been shifted +1 nm by a change in the dispersion of $\sim 10^{-4}$, which is within the accuracy claimed for the Sellmeier fit. The significance of this result is that the tuning curve shows a single well-defined peak with near theoretical bandwidth, demonstrating coherent interaction over the length of the sample.

For the 1.064-μm-pumped OPO, we fabricated another PPLN sample with a grating period of 31 μm, designed for nondegenerate operation at room temperature and tuning through degeneracy over a convenient temperature range. The finished device had a 5.2-mm interaction length with uniform domain pattern of quality comparable with that of the difference-frequency-generation piece shown in Fig. 1. The polished ends were antireflection coated for the 1.6–2.1-μm signal wavelength. The pump laser was a diode-pumped Q-switched Nd:YAG laser operating at 1.064 μm. The laser produced pulses with an energy of 2 mJ, a length of 7 ns FWHM, and a repetition rate of 100 Hz. The beam was slightly elliptical with a beam quality measure of $M^2 = 1.8$. The pump energy was varied with a half-wave plate and polarizer so that the pulse profile remained constant.

The OPO resonator was a linear cavity with mirror separation of 2 cm. The cavity was pumped through a mirror with 6.7-cm radius of curvature having a high-reflectivity coating for the signal wavelength that transmitted 94% of the pump and an average of 60% of the idler. The output coupler was a flat mirror that had an average reflectivity of 70% for the signal over the band of operation while transmitting 47% of the pump and 80% of the idler. Mode matching of the pump to the 103-μm cavity mode waist was not optimized; the actual pump beam radius in the crystal was 177 μm, and the waist occurred 16 mm past the cavity mode waist.

We tuned the signal (λ_S) and idler (λ_i) wavelengths continuously from 1.664 to 2.951 μm by heating the crystal to 180 °C, as shown in Fig. 3. The measured tuning curve agrees with that calculated from dispersion relationships[10] including the effect of thermal expansion. A difference in refractive index of

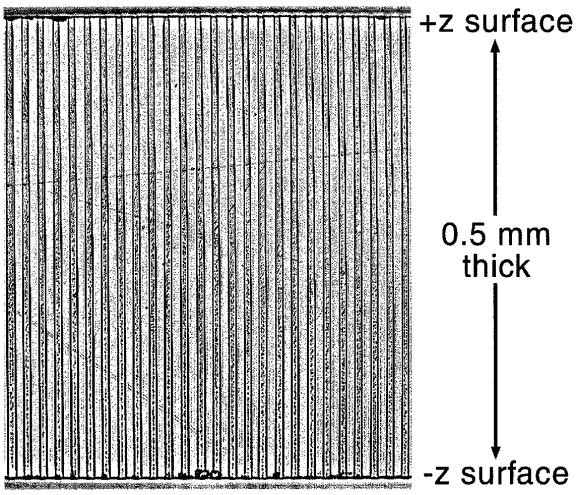

Fig. 1. Cross-sectional view (y face) of 0.5-mm-thick PPLN with a 15.5-μm period, after etching in HF acid to reveal the domain structure.

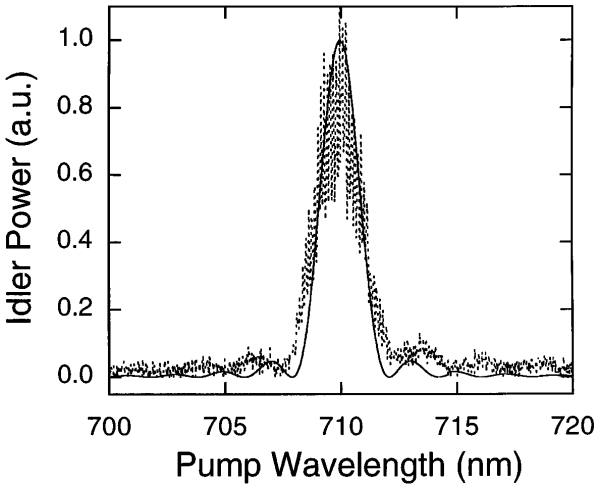

Fig. 2. Difference-frequency-generation tuning curve for 15.5-μm-period, 2.2-mm-long PPLN, with $\lambda_S = 1.555$ μm and $\lambda_i \approx 1.3$ μm. The calculated (solid) curve is based on the Sellmeier coefficients at 25 °C with the peak shifted +1 nm to match the data. The fringes in the data are due to Fresnel reflections from the uncoated end faces.

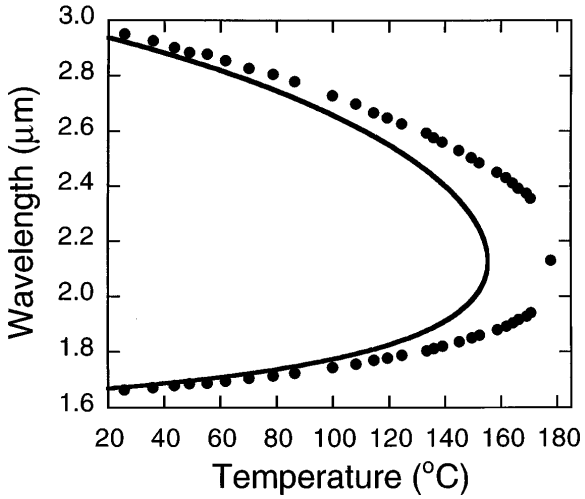

Fig. 3. Temperature tuning curve for 1.064-μm-pumped OPO in bulk PPLN with a 31-μm period. The calculated (solid) curve is based on the Sellmeier coefficients and includes thermal expansion. The offset between the data and theory is within the accuracy of the Sellmeier fit.

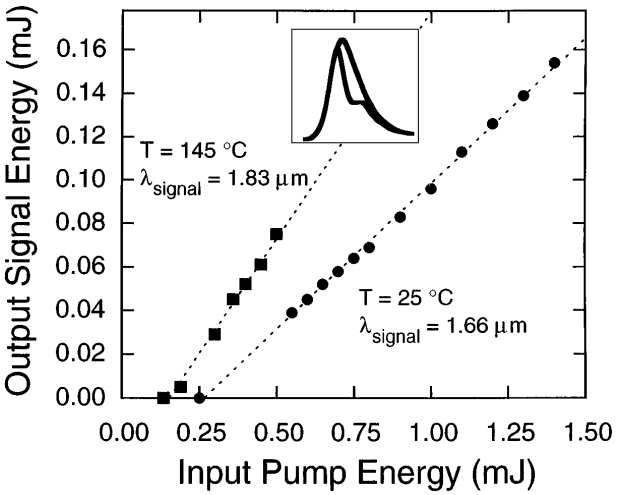

Fig. 4. OPO output signal energy versus input pump energy. The inset shows the time dependence of the incident and transmitted pump energy for a case with 25% depletion.

$<10^{-4}$, such as described above for the difference-frequency-generation experiment, could account for the offset between the calculated and measured tuning curves. The bandwidth of the signal, measured with a monochromator having a 2-nm resolution, was 6 nm at room temperature, increasing to 16 nm at 141 °C, which agrees with a theoretical calculation from the dispersion relationships.

The OPO threshold was 0.200 mJ at room temperature with $\lambda_S = 1.66$ μm and 0.135 mJ at 145 °C with $\lambda_S = 1.83$ μm as a result of lower cavity loss. We achieved threshold reduction to 0.080 mJ at 145 °C by replacing the output coupler with one that double passed the pump beam. These measurements agree with the calculated values that use a simplified model for a pulsed singly resonant oscillator,[11] indicating that the interaction was phase matched over the full device length and the loss was not noticeably increased over the bulk value. The output energy as a function of incident pump energy is shown in Fig. 4. At room temperature with $\lambda_S = 1.66$ μm, the slope efficiency was 14%, whereas at 145 °C with $\lambda_S = 1.83$ μm the slope efficiency was 22%. Pump depletion showed 24% photon conversion to the combined signal and idler wavelengths with pumping 1.9 times above threshold at 130 °C. By increasing the pump energy to intentionally damage the crystal, we obtained damage at 1.4 mJ or 3 J/cm^2, which agrees with previous reports for a single-domain $LiNbO_3$.[11] Improvements in performance are possible with optimization of material size, cavity design, and mode matching.

In summary, we have demonstrated a bulk QPM OPO that uses a 0.5-mm-thick, 5-mm-long PPLN crystal. This material has exceptional properties for bulk OPO applications. The loss and damage characteristics are comparable with their values in single-domain material. Devices prepared by our electric-field poling technique performed near theoretical expectations. The oscillation threshold is within the range of compact commercial diode-pumped Q-switched solid-state lasers and is a factor of 10 below the damage limit, important for practical devices. Scaling the device length to $\approx$1–2 cm should result in parametric gains for 1-μm pumping of $\sim$1%/W, suggesting cw singly resonant oscillator thresholds of a few watts and doubly resonant oscillator thresholds compatible with diode laser pump sources.

We thank M. L. Bortz for performing the difference-frequency-generation measurements and Crystal Technology, Inc., for supplying the $LiNbO_3$ wafers. This research was supported by the Advanced Research Projects Agency and the Office of Naval Research through the Center for Nonlinear Optical Materials at Stanford University. L. E. Myers acknowledges the support of the U.S. Air Force.

References

1. M. M. Fejer, G. A. Magel, D. H. Jundt, and R. L. Byer, IEEE J. Quantum Electron. **28,** 2631 (1992).
2. J. A. Armstrong, N. Bloembergen, J. Ducuing, and P. S. Pershan, Phys. Rev. **127,** 1918 (1962).
3. E. J. Lim, M. M. Fejer, and R. L. Byer, Electron. Lett. **25,** 174 (1989).
4. D. H. Jundt, G. A. Magel, M. M. Fejer, and R. L. Byer, Appl. Phys. Lett. **59,** 2657 (1991).
5. Y. Lu, L. Mao, and N. Ming, Opt. Lett. **19,** 1037 (1994).
6. H. Ito, C. Takyu, and H. Inaba, Electron. Lett. **27,** 1221 (1991).
7. M. Yamada, N. Nada, M. Saitoh, and K. Watanabe, Appl. Phys. Lett. **62,** 435 (1993).
8. W. K. Burns, W. McElhanon, and L. Goldberg, IEEE Photon. Technol. Lett. **6,** 252 (1994).
9. J. Webjörn, V. Pruneri, P. St. J. Russell, J. R. M. Barr, and D. C. Hanna, Electron. Lett. **30,** 894 (1994).
10. G. J. Edwards and M. Lawrence, Opt. Quantum Electron. **16,** 373 (1984).
11. S. J. Brosnan and R. L. Byer, IEEE J. Quantum Electron. **QE-15,** 415 (1979).